Model for spin relaxation by correlated internal motions in liquid crystals

Ronald Y. Dong
Department of Physics and Astronomy, Brandon University, Brandon, Manitoba, Canada R7A 6A9
(Received 22 May 1990)

The effects of correlated internal rotations in an alkyl chain on the spectral densities of motion in liquid crystals are examined using the master-equation method. It is assumed that the overall reorientation of molecules is decoupled from the internal motions in their alkyl end chains. The pentyl chain that is attached to a cylindrical biphenyl core in 4-*n*-pentyl-4′-cyanobiphenyl (5CB) is studied as a specific example. The reorientation of a symmetric top in an anisotropic potential is described by the small-step rotational diffusion model. The equilibrium probability of each conformer, which is required to construct the transition-rate matrix for the master equation, is obtained using the Emsley-Luckhurst theory. The effects of the nematic mean field on the chain dynamics are discussed. Both $J_1(\omega)$ and $J_2(2\omega)$ in 5CB are found to be frequency dependent, with $J_2(2\omega)$ being weaker.

I. INTRODUCTION

Recent interest in measurement of spectral densities of motion[1–4] by means of deuterium nuclear magnetic resonance (NMR) relaxation study in deuteriated liquid crystals has yielded a wealth of experimental data that has allowed testing of motional models that describe reorientation and internal motions of molecules oriented in an ordering pseudopotential. Multiple internal rotations within flexible molecules have been studied by many authors at varying levels of treatment. Wallach[5] considers internal rotations assuming that free diffusive rotations about the various carbon-carbon bonds occur and all the rotations are independent. Levine *et al.*[6] have extended this approach by using a single phenomenological rate constant for the internal rotations. The assumption of free rotations can give conformations of molecules that are precluded on grounds of "excluded-volume" effects, while the decoupled rotations are inapplicable to long chain molecules because the large change in the molecular shape may not be favored by the intermolecular forces. Despite these drawbacks, a superimposed rotations model is used by Beckmann *et al.*[1] in an attempt to describe internal motions of an alkyl chain in a nematogen. The Wallach approach was later improved by the jump model. Assuming decoupled internal rotations, London and Avitabile[7] explicitly consider the energetics of the trans-gauche isomerism based on the rotational isometric state (RIS) model.[8] This has been refined[9] by Tsutsumi. Wittebort and Szabo[10] consider concerted internal rotations by explicitly following conformational transitions through a master equation. They use phenomenological transition rates for one-bond, two-bond, and three-bond motions in a side chain attached to a macromolecule which diffuses as a symmetric top in solution. Edholm and Blomberg[11] apply the Kramer's formula to the case of conformational processes. A multidimensional diffusion equation has recently been applied[12] to describe motion of aliphatic tails in isotropic solutions.

Following Tsutsumi, a jump model is used[13] to discuss internal dynamics of liquid crystals. The spectral densities calculated using this decoupled jump model make numerical computation difficult unless only one bond is allowed to jump. In order to model correlated internal rotations in a mesogen, we extend the master-equation method[10] to flexible cylindrical molecules reorienting in an anisotropic potential of mean torque. The equilibrium probability of a rotamer is calculated based on the Emsley-Luckhurst theory,[14] which has been successfully used to explain equilibrium properties such as quadrupolar splittings observed in deuteriated liquid crystals. Several models[15–17] have been used to describe reorientation of rigid molecules in an ordering potential of Maier-Saupe type. The small-step rotational diffusion model[15] is used here, since it has been successful in interpreting data obtained in liquid crystals by various experimental techniques[18] including NMR. In this model, molecular reorientation is governed by a rotational diffusion tensor that is diagonal in a molecule-fixed frame. In a flexible molecule with N distinct conformations, we assume that diffusion tensors for different rotamers do not differ appreciably and that an "average" rotational diffusion tensor may be used to solve the rotational diffusion equation. In this paper, we propose a simple theory[19] based on the master-equation method to describe correlated internal motions in liquid crystals. This provides the theoretical background necessary for gaining insight into internal dynamical processes in anisotropic media.

II. THEORY

The nuclear spin-relaxation rates are given as linear combinations of spectral densities of motion $J_{m_L}(m_L\omega)$ which may be evaluated by Fourier transforming the time autocorrelation functions of fluctuation interactions. In the case of deuteron ($I=1$) with nuclear quadrupolar interaction[20] being the dominant interaction,

$$J_{m_L}(m_L\omega)=\frac{3\pi^2}{2}(\nu_Q)^2\int_0^\infty G_{m_L}(t)\cos(m_L\omega t)dt \ , \quad (1)$$

where $\nu_Q=e^2qQ/h$, the quadrupolar coupling constant ($\eta=0$ is assumed) and the time autocorrelation function

$$G_{m_L}(t)=\langle D^2_{m_L0}(\Omega_{LQ}(0))D^{2*}_{m_L0}(\Omega_{LQ}(t))\rangle \ , \quad (2)$$

where the Euler angles Ω_{LQ} specify the orientation of principal axes of the electric-field-gradient tensor with respect to the external magnetic field. To evaluate $G_{m_L}(t)$, one needs to transform the electric-field-gradient tensor through successive coordinates to allow for internal motions and reorientation of the molecule. We define a coordinate system (N) in which the chain may have N distinct configurations. The N frame is attached rigidly on a molecule-fixed (M) frame with an orientation specified by the time-independent Euler angles Ω_{MN}. In each configuration, a C—D bond has a known orientation. Its motion due to conformational transitions is responsible for spin relaxation. Using the decomposition theorem for the Wigner matrix components, one has

$$D^2_{m_L0}(\Omega_{LQ})=\sum_{m_M,m_\alpha} D^2_{m_Lm_M}(\Omega_{LM})D^2_{m_Mm_\alpha}(\Omega_{MN})\times D^2_{m_\alpha0}(\Omega_{NQ}) \ , \quad (3)$$

where the Euler angles Ω_{LM} give the orientation of the M frame with respect to the laboratory (L) frame (Z_L axis $\|\mathbf{B}$), while Ω_{NQ} give the orientation of the C—D bond in the N frame. Both Ω_{LM} and Ω_{NQ} are time dependent because of molecular reorientation and internal motion, respectively. It is conventional to assume that internal motion is independent of the overall reorientation of the molecule. With this assumption and if the rotational motion about the Z_M axis has cylindrical symmetry,

$$G_{m_L}(t)=\sum_{m_M}\sum_{m_\alpha}\sum_{m'_\alpha} D^2_{m_Mm_\alpha}(\Omega_{MN})D^{2*}_{m_Mm'_\alpha}(\Omega_{MN})\times[g_{m_Lm_M}(t)\langle D^2_{m_\alpha0}(\Omega_{NQ}(0))D^{2*}_{m'_\alpha0}(\Omega_{NQ}(t))\rangle+(\bar{P}_2)^2\delta_{m_M0}\delta_{m_L0}\langle D^2_{m_\alpha0}(\Omega_{NQ}(0))D^{2*}_{m'_\alpha0}(\Omega_{NQ}(t))\rangle] \ , \quad (4)$$

where $\bar{P}_2$ is the orientational order parameter, and $g_{m_Lm_M}(t)$, the correlation functions that describe the reorientation of a molecule, are given by

$$g_{m_Lm_M}(t)=\langle D^2_{m_Lm_M}(\Omega_{LM}(0))D^{2*}_{m_Lm_M}(\Omega_{LM}(t))\rangle-\langle D^2_{m_Lm_M}(\Omega_{LM})\rangle\langle D^{2*}_{m_Lm_M}(\Omega_{LM})\rangle \ , \quad (5)$$

while $\langle D^2_{m_\alpha0}(\Omega_{NQ}(0))D^{2*}_{m'_\alpha0}(\Omega_{NQ}(t))\rangle$ are internal correlation functions that describe internal motion of the chain with respect to the N frame. The second term in Eq. (5), which is equal to the first one at $t=\infty$, makes the correlation function $g_{m_Lm_M}(t)$ decay to zero, so that only the fluctuating part of the interaction remains. Using the assumption of decoupling internal and external motions, the conditional probability that at time t, the molecule has configuration i and orientation Ω_{LM} and when at $t=0$, the molecule has configurational l and $\Omega_{LM}(0)$ can be expressed as the product of configuration and orientation conditional probabilities:

$$p_{il_0}(\Omega_{LM},t|\Omega_{LM}(0),0)=p(i,t|l,0)p(\Omega_{LM},t|\Omega_{LM}(0),0) \ . \quad (6)$$

The thermal average in Eq. (2) can be evaluated by using the conditional probability to give

$$G_{m_L}(t)=\sum_{i,l}\int\int d\Omega_{LM}d\Omega_{LM}(0)D^2_{m_L0}(\Omega_{LQ}(0))\times D^{2*}_{m_L0}(\Omega_{LQ}(t))p_{\rm eq}(l)p_{il_0}(\Omega_{LM},t|\Omega_{LM}(0),0) \ , \quad (7)$$

where $p_{\rm eq}(l)$ is the probability of occurrence of configuration l at equilibrium. $g_{m_Lm_M}(t)$ has been given by the small-step rotational diffusion model[15,17]

$$g_{m_Lm_M}(t)=c_{m_Lm_M}\sum_k a^{(k)}_{m_Lm_M}\exp(-t/\tau^{(k)}_{m_Lm_M}) \ , \quad (8)$$

where $c_{m_Lm_M}$ represents the initial amplitude of the correlation function and is given by the mean square of the Wigner rotation matrices. $a^{(k)}_{m_Lm_M}$ represent normalized weights of each exponetial decay with time constant $\tau^{(k)}_{m_Lm_M}$,

$$\tau^{(k)}_{m_Lm_M}=b^{(k)}_{m_Lm_M}\tau^{(2)}_{m_M}=b^{(k)}_{m_Lm_M}/[6D_\perp+m^2_M(D_\|-D_\perp)] \ . \quad (9)$$

$\tau^{(2)}_{m_M}$ are the usual correlation times for diffusion of molecules in an isotropic medium and are given in terms of $D_\|$ and $D_\perp$, rotational diffusion constants of the molecule about its Z_M axis and of the Z_M axis, respectively. The a, b, and c coefficients are all depending on $\bar{P}_2$, and are tabulated for the Maier-Saupe potential in Table I of Ref. 17. Equation (8) is obtained by performing the double integrals in Eq. (7) with $p(\Omega_{LM},t|\Omega_{LM}(0),0)$ solved from the rotational diffusion equation of a symmetric top in a Maier-Saupe potential. Now the internal correlation functions in Eq. (4) are given by

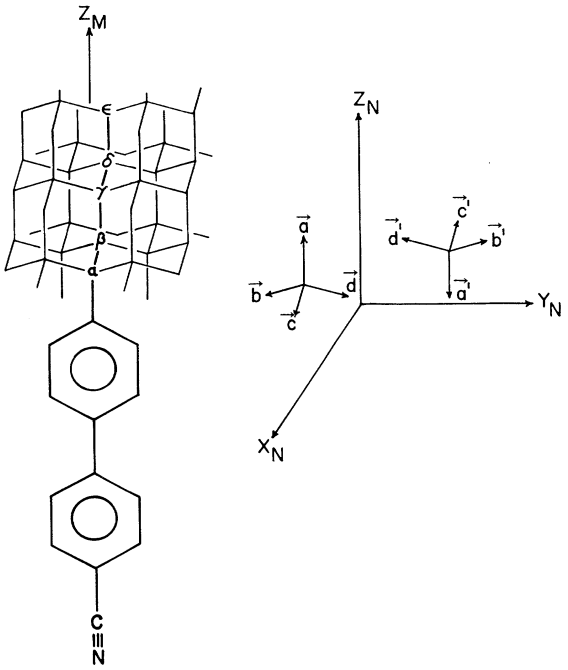

FIG. 1. The tetrahedral lattice on which the pentyl chain backbone of a 5CB molecule is constrained. The eight possible orientations of a vector connecting two lattice points and the M and N frames are shown. The vectors **c** and **c'** lie on the $X_N Z_N$ plane.

TABLE I. Euler angles for the tetrahedral lattice vectors.

Lattice vector	β_{NQ}	α_{NQ}
a	0	
b	109.5	−120
c	109.5	0
d	109.5	+120
a'	180	
b'	70.5	60
c'	70.5	180
d'	70.5	300

$$\langle D^2_{m_\alpha 0}(\Omega_{NQ}(0)) D^{2*}_{m'_\alpha 0}(\Omega_{NQ}(t))\rangle = \sum_{i,l} \exp(-im_\alpha \alpha^l_{NQ}) d^2_{m_\alpha 0}(\beta^l_{NQ}) p_{\rm eq}(l) \times \exp(im'_\alpha \alpha^i_{NQ}) d^2_{m'_\alpha 0}(\beta^i_{NQ}) p(i,t|l,0) , \quad (10)$$

where β^i_{NQ} and α^i_{NQ} are the polar angles of the C—D bond in the rotamer of configuration i in the N frame.

To evaluate internal correlation functions, one requires both $p_{\rm eq}(l)$ and $p(i,t|l,0) \equiv p_{i,l_0}$. For simplicity, we adopt the diamond (tetrahedral) lattice to describe the carbon-carbon backbone of an alkyl chain and the bond lengths of C—C and C—D bond are assumed to be identical. There are eight possible orientations of a vector connecting two adjacent points on the lattice. These belong to the antiparallel sets {**a**,**b**,**c**,**d**} and {**a'**,**b'**,**c'**,**d'**}, as indicated in Fig. 1. Table I gives the Euler angles for the tetrahedral lattice vectors. The Z_N axis is in the **a** direction. There are N distinct configurations for the chain. Transitions between different configurations take place by means of one-bond, two-bond, or three-bond motion[21] in the chain. These bond motions involve jump rate constants k_1, k_2, and k_3, respectively. In general, for each type of bond motion, one needs more than one rate constant to account for the difference in number of gauche linkages in conformations. Transitions among configurations are described by a master equation,

$$\frac{\partial p_{il_0}(t)}{\partial t} = \sum_{j=1}^{N} R_{ij} p_{jl_0}(t) , \quad (11)$$

where R_{ij} is the rate constant for transition from configuration j to configuration i. This depends on the type of bond motion in the transition. The diagonal matrix elements of $\bar{R}$ are the negative of sum of all rates which deplete configuration i,

$$R_{ii} = -\sum_{j\neq i} R_{ji} . \quad (12)$$

Moreover, R_{ij} satisfy the detailed-balance principle,

$$R_{ij} p_{\rm eq}(j) = R_{ji} p_{\rm eq}(i) . \quad (13)$$

Equation (11) has been solved[10] as an eigenvalue problem. This is achieved by symmetrizing $\bar{R}$ and then diagonalizing to give N real and negative eigenvalues λ_n and eigenvectors $\mathbf{x}^n$. One of these eigenvalues ($n=1$) is zero, and the corresponding eigenvector $\mathbf{x}^{(1)}$ is given by the equilibrium distribution of configuration, i.e., $x^{(1)}_l = [p_{\rm eq}(l)]^{1/2}$. The conditional probability $p_{il_0}(t)$ is given by

$$p_{il_0}(t) = x^{(1)}_i (x^{(1)}_l)^{-1} \sum_{n=1}^{N} x^{(n)}_i x^{(n)}_l \exp(-|\lambda_n| t) . \quad (14)$$

Using Eq. (14) in Eq. (10), one obtains

$$\langle D^2_{m_\alpha 0}(\Omega_{NQ}(0)) D^{2*}_{m'_\alpha 0}(\Omega_{NQ}(t))\rangle = \sum_{n=1}^{N} \exp(-|\lambda_n| t) \left| \sum_{l=1}^{N} d^2_{m_\alpha 0}(\beta^l_{NQ}) \exp(-im_\alpha \alpha^l_{NQ}) x^{(1)}_l x^{(n)}_l \right|^2 . \quad (15)$$

We consider here the pentyl chain of 4-n-pentyl-d_{11}-4'-cyanobiphenyl-d_4 (5CB-d_{15}). The biphenyl core is assumed to possess cylindrical symmetry. The M frame can be chosen to be identical to the N frame (see Fig. 1), whose X_N axis is picked such that the **c** and **c'** directions lie on the $X_N Z_N$ plane. Substituting Eqs. (8) and (15) into Eq. (4), one obtains

$$G_{m_L}(t)=\sum_{m_M} c_{m_L m_M}\sum_{n=1}^{N}\sum_{k} a^{(k)}_{m_L m_M}\left|\sum_{l=1}^{N} d^2_{m_M 0}(\beta^l_{MQ})\exp(-im_M\alpha^l_{MQ})x^{(1)}_l x^{(n)}_l\right|^2 \exp\{-[(\tau^{(k)}_{m_L m_M})^{-1}+|\lambda_n|]t\}$$
$$+\delta_{m_L 0}(\bar{P}_2)^2\sum_{n=1}^{N}\left|\sum_{l=1}^{N} d^2_{00}(\beta^l_{MQ})x^{(1)}_l x^{(n)}_l\right|^2 \exp(-|\lambda_n|t)\ . \tag{16}$$

The spectral densities $J^{(p)}_{m_L}(m_L\omega)$ of the deuterons on the C_p carbon are calculated from Eq. (1):

$$J^{(p)}_{m_L}(m_L\omega)=\frac{3\pi^2}{2}(\nu^{(p)}_Q)^2\sum_{m_M}\sum_{n=1}^{N} c_{m_L m_M}\left|\sum_{l=1}^{N} d^2_{m_M 0}(\beta^{(p)l}_{MQ})\exp(-im_M\alpha^{(p)l}_{MQ})x^{(1)}_l x^{(n)}_l\right|^2$$
$$\times\sum_{k} a^{(k)}_{m_L m_M}[(\tau^{(k)}_{m_L m_M})^{-1}+|\lambda_n|]/\{(m_L\omega)^2+[(\tau^{(k)}_{m_L m_M})^{-1}+|\lambda_n|]^2\}$$
$$+\frac{3\pi^2}{2}(\nu^{(p)}_Q)^2\delta_{m_L 0}(\bar{P}_2)^2\sum_{n=1}^{N}\left|\sum_{l=1}^{N} d^2_{00}(\beta^{(p)l}_{MQ})x^{(1)}_l x^{(n)}_l\right|^2 |\lambda_n|/[(m_L\omega)^2+|\lambda_n|^2]\ . \tag{17}$$

Since we are concerned with $m_L\neq 0$ in the Zeeman and quadrupolar spin-lattice relaxation times, the second term involving $\bar{P}_2{}^2$ in the above equation will subsequently be omitted.

To construct the rate matrix $\tilde{R}$ in the master equation, the elementary jump modes connecting the configurations and the equilibrium probability $p_{\rm eq}(j)$ of the configuration j must be specified. To obtain $p_{\rm eq}(j)$ for a free alkyl chain, one needs only the intramolecular energy $U_{\rm int}(j)$. This can be approximated by $U_{\rm int}(j)=n_g E_{tg}$, where n_g is the number of gauche linkages in the chain in configuration j and E_{tg} is the energy difference between the $g^{\pm}$ state and the t state. E_{tg} varies between 2.1 and 3.2 kJ/mol in gaseous alkanes. A slightly larger value[14] was used in liquid crystals. The total energy $U(j,\omega)$ of a molecule in configuration j, having an orientation ω with the director, is given by sum of $U_{\rm int}(j)$ and $U_{\rm ext}(j,\omega)$, the anisotropic part of the potential of mean torque. It can be shown[14] that $p_{\rm eq}(j)$ is given by

$$p_{\rm eq}(j)=\exp[-U_{\rm int}(j)/kT]Q_j/Z\ , \tag{18}$$

where the orientational partition function for configuration j is

$$Q_j=\int\exp[-U_{\rm ext}(j,\omega)/kT]d\omega\ , \tag{19}$$

and the configuration-orientational partition function Z is

$$Z=\sum_{j=1}^{N}\exp[-U_{\rm int}(j)/kT]Q_j\ . \tag{20}$$

The $U_{\rm ext}(j,\omega)$ for configuration j can be written[14] as

$$U_{\rm ext}(j,\omega)=-[X^j_{20}P_2(\cos\beta)+2X^j_{22}d^2_{20}(\beta)\cos 2\gamma]\ , \tag{21}$$

where (β,γ) are the polar angles of the director in the principal frame of the interaction tensor $\tilde{X}$. An extended-atom model is assumed for the chain, with only the skeleton carbons being explicitly considered. The $\tilde{X}$ is obtained based on additivity of local-bond-interaction tensors which are cylindrically symmetric and independent of configuration. Therefore

$$X^j_{2,m}=X_a\delta_{m0}+X_{\rm CC}\sum_{i=2}^{5} C_{2,m}(\omega^j_i)\ , \tag{22}$$

where ω^j_i is the orientation of the ith C-C segment in the molecular (M) frame for configuration j, $C_{2,m}(\omega)$ is a modified spherical harmonic, X_a and $X_{\rm CC}$ are the unique components of the interaction tensors for the aromatic core (including the cyano group and the first methylene group) and for a C-C segment, respectively. $\tilde{X}$ is a 3×3 matrix and is diagonalized to determine the X^j_{20} and X^j_{22} in Eq. (21). X_a and $X_{\rm CC}$ can be derived from fitting the quadrupolar splittings of the chain deuterons, and are temperature dependent.[22] They are assumed to be known in modeling dynamics of the chain.

The elementary jump modes are defined[21] by Monnerie and co-workers. Any configuration of the pentyl chain can be written as a sequence of five lattice vectors {**ij'kl'm**} representing the orientations of C_{ar}-C_α, C_α-C_β, C_β-C_γ, C_γ-C_δ, and C_δ-C_ϵ, respectively. For example, the configuration illustrated in Fig. 1 is specified by the set of vectors {**ac'ac'a**}. To construct all possible sterically allowed configurations, only those sequences {**ij'kl'm**} are allowed in which adjacent vectors, disregarding the primes, are different. As the C_{ar}—C_α bond is fixed on the aromatic core, i can only take one possible value which is taken to be **a**, and the pentyl chain could have 3^{5-1} configurations. In addition, four bond sequences that contain a $g^{\pm}g^{\mp}$ conformation are disallowed because deuteron and deuteron or carbon atoms would occupy the same lattice site in the case that C—C and C—D bond lengths were exactly the same. These **j'kl'm** sequences are given by **j**=**m**. As a result, the number of acceptable configurations N is reduced to 51. The 21 configurations[10] of the type {**aj'al'm**} are listed in Table II(a). The ten configurations of the type {**aj'cl'm**} are listed in Table II(b). There are ten configurations of the type {**aj'dl'm**} and of the type {**aj'bl'm**}. These can be generated in the same manner as those given in Table II(b). To evaluate the spectral density of a deuteron, the

orientation of the C-D vector in each of the configurations, which have been specified in terms of the carbon-carbon skeleton, must be known. A C-D vector may only have one of eight possible orientations in a diamond lattice, i.e., {**a**,**b**,**c**,**d**} and {**a**′,**b**′,**c**′,**d**′}. There are two sets of C-D vectors, each of which contains one of the two deuterons bonded to each carbon. We follow Wittebort and Szabo[10] by assigning {**c**′,**c**,**c**′,**c**}=set 1 and {**b**′,**b**,**b**′,**b**}=set 2 for configuration {**ad**′**ad**′**a**}. Only set 1 of C-D vectors is given in Table II, as the spectral density is independent of whether set 1 or set 2 is used. With the above assignment, the C-D vectors in all the other configurations are determined as follows. Consider a chain which starts in configuration 1 and makes a jump to another configuration by a possible elementary motion. The accompanying changes in the directions of the C-D vectors can be determined[10] using the following rule: any C-D vector attached to a C—C bond which moves must alter its orientation.

The interconversions among the configurations are governed by the rate matrix elements R_{ij} involving elementary jump constants. The elementary jump modes in $\tilde{R}$ are presented in graphical form in terms of one-bond, two-bond, and three-bond motions in Fig. 2. The three-bond motions involve

$$\mathbf{ij'kl'm} \overset{k_3}{\rightarrow} \mathbf{il'kj'm} , \tag{23}$$

e.g., **ad**′**ab**′**a**→**ab**′**ad**′**a** ($tg^-t \rightarrow tg^+t$). However, not all three-bond motions are equivalent. The jump rates for **ad**′**cb**′**a**→**ab**′**cd**′**a** ($g^+g^+g^+ \rightarrow g^-g^-g^-$), **ad**′**cb**′**c**→**ab**′**cd**′**c** ($g^+g^+t \rightarrow g^-g^-t$), and **ad**′**ab**′**a**→**ab**′**ad**′**a** are slightly different from each other. For simplicity, these rates are assumed to identical. The two-bond motions are of the type

$$\mathbf{ij'kl'm} \overset{k_2}{\rightarrow} \mathbf{ij'kn'm} , \tag{24}$$

while one-bond motions are of the type

$$\mathbf{ij'kl'm} \overset{k_1}{\rightarrow} \mathbf{ij'kl'n} , \tag{25}$$

which involve rotation about the C_γ—C_δ bond. Not all one-bond motions are equivalent. For example,

TABLE II. Configurations, conformations, and C-D vectors (set 1) of a pentyl chain.

No.	Conformation	Configuration					C-D vectors C_α	C_β	C_γ	C_δ
				(a)						
1	ttt	a	d′	a	d′	a	c′	c	c′	c
2	ttg^+	a	d′	a	d′	c	c′	c	c′	b
3	ttg^-	a	d′	a	d′	b	c′	c	c′	a
4	tg^+t	a	d′	a	c′	a	c′	c	b′	b
5	tg^-t	a	d′	a	b′	a	c′	c	d′	d
6	tg^+g^+	a	d′	a	c′	b	c′	c	b′	d
7	tg^-g^-	a	d′	a	b′	c	c′	c	d′	a
8	ttt	a	b′	a	b′	a	d′	d	d′	d
9	ttg^+	a	b′	a	b′	d	d′	d	d′	c
10	ttg^-	a	b′	a	b′	c	d′	d	d′	a
11	tg^+t	a	b′	a	d′	a	d′	d	c′	c
12	tg^-t	a	b′	a	c′	a	d′	d	b′	b
13	tg^+g^+	a	b′	a	d′	c	d′	d	c′	b
14	tg^-g^-	a	b′	a	c′	d	d′	d	b′	a
15	ttt	a	c′	a	c′	a	b′	b	b′	b
16	ttg^+	a	c′	a	c′	b	b′	b	b′	d
17	ttg^-	a	c′	a	c′	d	b′	b	b′	a
18	tg^+t	a	c′	a	b′	a	b′	b	d′	d
19	tg^-t	a	c′	a	d′	a	b′	b	c′	c
20	tg^+t^+	a	c′	a	b′	d	b′	b	d′	c
21	tg^-g^-	a	c′	a	d′	b	b′	b	c′	a
				(b)						
22	g^+tt	a	d′	c	d′	c	c′	b	b′	b
23	g^+tg^-	a	d′	c	d′	a	c′	b	b′	c
24	g^+tg^+	a	d′	c	d′	b	c′	b	b′	a
25	g^+g^+t	a	d′	c	b′	c	c′	b	a′	a
26	$g^+g^+g^+$	a	d′	c	b′	a	c′	b	a′	d
27	g^-tt	a	b′	c	b′	c	d′	a	a′	a
28	g^-tg^+	a	b′	c	b′	a	d′	a	a′	d
29	g^-tg^-	a	b′	c	b′	d	d′	a	a′	c
30	g^-g^-t	a	b′	c	d′	c	d′	a	b′	b
31	$g^-g^-g^-$	a	b′	c	d′	a	d′	a	b′	c

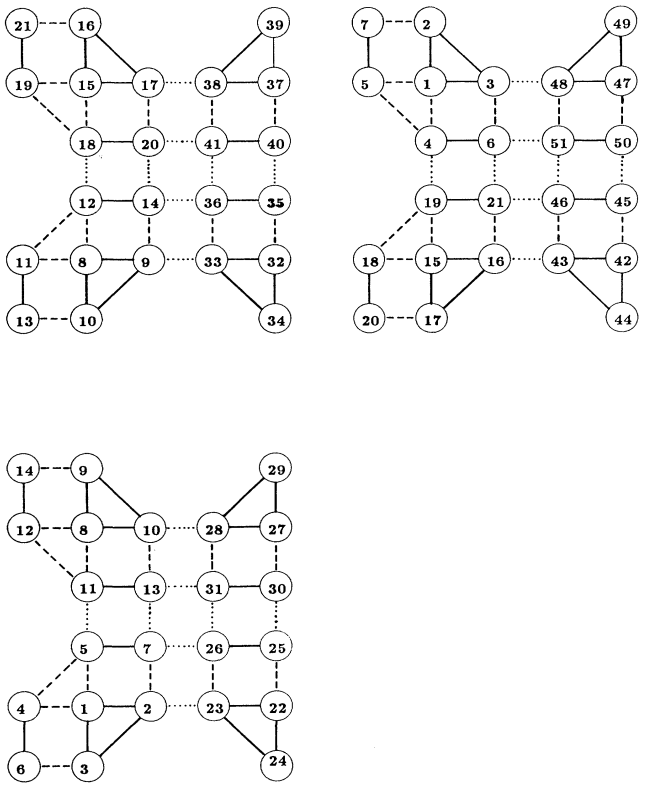

FIG. 2. Diagrammatic representation of the rate matrix $\tilde{R}$. The jump rate constants are k_1 (solid line), k_2 (dashed line), and k_3 (dotted line).

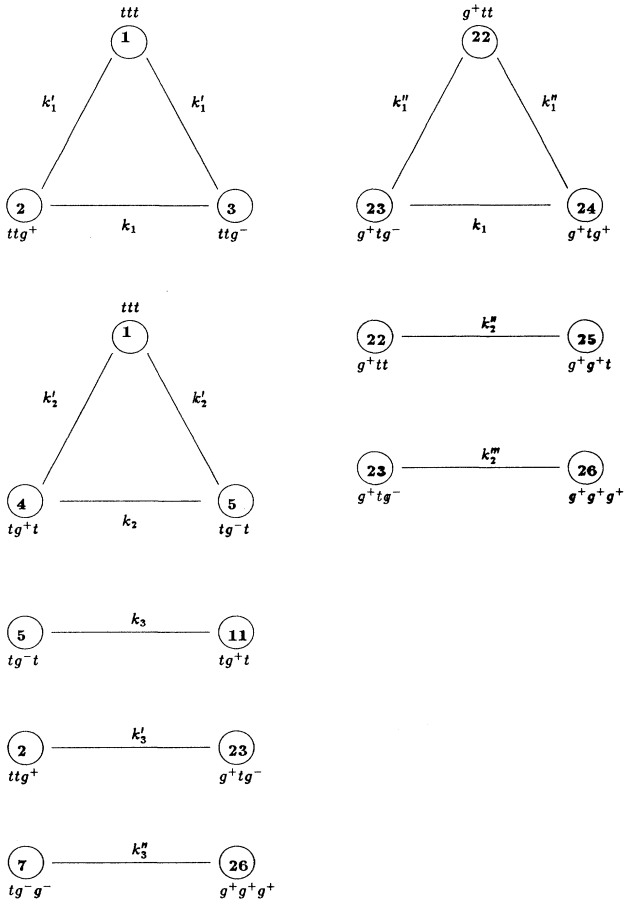

FIG. 3. Generalization of a part of the rate matrix $\tilde{R}$ in Fig. 2 to the case of nonuniform equilibrium distribution of the configurations.

ad'ad'c→ad'ad'b and **ad'cd'a→ad'cd'b** have slightly different rate constants. Again they are set to the same value for simplicity. Because of Eq. (13) and the elementary jump rate constants $r_{ij}=r_{ji}$, $R_{ij}=p_{\rm eq}(i)r_{ij}$. In general, more than one rate constant for each type of bond motion is needed because of different internal energies $U_{\rm int}(j)$ involved in the interconversion among configurations. For example, the interconversions between configurations 1, 2, and 3 involve one-bond motions. If we define k_1 to be the rate constant for transition between two conformations which have an equal number of gauche sequences, an additional rate k_1' is needed (Fig. 3) for transition between configuration 1 and configuration 2 or 3. Also shown in this figure are some examples of various rates for two- and three-bond motions. These are required to determine r_{ij} in Table III.

We summarize how the spectral density is calculated using the information in Tables II and III and Eq. (17). The 51×51 rate matrix $\tilde{R}$ is constructed and then symmetrized. This is followed by diagonalization using standard routines[23] to yield a set of eigenvalues λ_n and corresponding eigenvectors $x_i^{(n)}$ $(i,n=1,\ldots,51)$. To evaluate the spectral density of deuterons on any carbon except C_ϵ, the required polar angles α_{NQ} and β_{NQ} for each deuteron in each configuration are obtained using both Tables I and II. To obtain the orientation of the C-D vector in the methyl $(p=\epsilon)$ group, it is assumed that the threefold rotation of the methyl group is fast, thus making the "effective" C-D vector identical to the C_δ-C_ϵ vector and reducing $\nu_Q^{(\epsilon)}$ by a factor of $P_2(\cos\theta)$, where θ is the ∠CCD (109.5°) in the methyl group.

Finally, the spectral densities for the ring deuterons are obtained using the superimposed free-rotation model[24]

$$J_{m_L}^{(R)}(m_L\omega)=\frac{3\pi^2}{2}(\nu_Q^{(R)})^2\sum_{m_M}c_{m_Lm_M}[d^2_{m_M0}(\beta_{M,Q})]^2 \times\sum_j a^{(j)}_{m_Lm_M}[(\tau^{(j)}_{m_Lm_M})^{-1}+(1-\delta_{m_M0})D_R]/\{(m_L\omega)^2+[(\tau^{(j)}_{m_Lm_M})^{-1}+(1-\delta_{m_M0})D_R]^2\}\ , \quad (26)$$

TABLE III. Elementary rate constants required to construct the rate matrix $\bar{R}$. Only the nonzero r_{ij} (for $j>i$) are listed. Under each column of rate constant are the indices (i,j) of r_{ij}.

k_1	k_1'	k_1''	k_1'''	k_2	k_2'	k_2''	k_2'''	k_3	k_3'	k_3''
(2,3)	(1,2)	(4,6)	(25,26)	(4,5)	(1,4)	(2,7)	(23,26)	(4,19)	(2,23)	(6,51)
(9,10)	(1,3)	(5,7)	(30,31)	(11,12)	(1,5)	(3,6)	(28,31)	(5,11)	(3,48)	(7,26)
(16,17)	(8,9)	(11,13)	(35,36)	(18,19)	(8,11)	(9,14)	(33,36)	(6,21)	(9,33)	(13,31)
(23,24)	(8,10)	(12,14)	(40,41)		(8,12)	(10,13)	(38,41)	(7,13)	(10,28)	(14,36)
(28,29)	(15,16)	(18,20)	(45,46)		(15,18)	(16,21)	(43,46)	(12,18)	(16,43)	(20,41)
(33,34)	(15,17)	(19,21)	(50,51)		(15,19)	(17,20)	(48,51)	(14,20)	(17,38)	(21,46)
(38,39)		(22,23)				(22,25)		(25,30)		
(43,44)		(22,24)				(27,30)		(26,31)		
(48,49)		(27,28)				(32,35)		(35,40)		
		(27,29)				(37,40)		(36,41)		
		(32,33)				(42,45)		(45,50)		
		(32,34)				(47,50)		(46,51)		
		(37,38)						(24,29)		
		(37,39)						(29,34)		
		(42,43)						(39,44)		
		(42,44)								
		(47,48)								
		(47,49)								

where D_R is the rotational diffusion constant of the ring about its para axis. A strong collision limit is assumed for the free internal ring rotation. $\nu_Q^{(R)}=185$ kHz, while $\nu_Q^{(p)}$ for the methylene deuteron is taken to be 168 kHz. In the next section we examine the site, temperature, and frequency dependences of $J_1(\omega_0)$ and $J_2(2\omega_0)$ in the deuterated liquid crystal 5CB-d_{15} using Eqs. (17) and (26).

III. NUMERICAL CALCULATIONS

Using the above jump model, we present some numerical calculations of spectral densities for the pentyl chain of 5CB and qualitatively compare the theoretical predictions and the experimental data.[1] The parameters in the potential of mean torque are taken from Counsell *et al.*[22] At $T=302$ K, $X_a=4.52$ kJ/mol and $X_{CC}=1.36$ kJ/mol. While a value of 3.27 kJ/mol was used for E_{tg} in 5CB by Cheng and Dong,[14] E_{tg} was taken to be 3.8 kJ/mol by Counsell *et al.* Using $\bar{P}_2=0.533$, $E_{tg}=3.5$ kJ/mol, $D_{\parallel}=7.6\times10^8$ s^{-1}, $D_{\perp}=4.5\times10^7$ s^{-1}, and $D_R=2.2\times10^9$ s^{-1}, $J_1^{(R)}(\omega_0)$ and $J_2^{(R)}(2\omega_0)$ at $\omega_0/2\pi=30.7$ MHz are calculated from Eq. (26) to be 36.06 and 25.77 s^{-1}, respectively. We have chosen the rotational diffusion constants so that these theoretical values are close to the experimental spectral densities[1] at this temperature ($J_1=36.7\pm1.8$ s^{-1} and $J_2=25.1\pm2.5$ s^{-1}). Following Wittebort and Szabo,[10] all phenomenological rate constants in $\bar{R}$ are set equal. Thus the spectral densities for deuterons at all carbons in the pentyl chain of 5CB may be calculated with only one adjustable parameter k (i.e., the jump rates for one-, two-, and three-bond motions are set to be identical).

It has been shown[25] that conformational dynamics appear to be relatively insensitive to the presence of an anisotropic potential of mean torque in systems like lipid bilayers. To investigate this possibility in liquid crystals, the spectral densities for a free pentyl chain are calculated using

$$p_{eq}(j)=\exp[-U_{int}(j)/kT]/\sum_{j=1}^{N}\exp[-U_{int}(j)/kT] \tag{27}$$

and Eq. (17). Figure 4 shows plot of calculated $J_1^{(p)}(\omega_0)$ and $J_2^{(p)}(2\omega_0)$ and $\omega_0/2\pi=30.7$ MHz versus the carbon number with $k=6\times10^{12}$ s^{-1}. The model predicts a decrease in both J_1 and J_2 along the pentyl chain except at C(5). For comparison, we have also plotted in the same diagram the calculated spectral densities with the same motional parameters and $p_{eq}(j)$ given by Eq. (18). The above k value was chosen to give qualitative agreement between the calculated spectral densities for a constrained chain and the experimental data.[1] As seen from the figure, the effects of the nematic mean field on the internal dynamics of a chain appear not be significant for liquid crystals, since these spectral densities are only slightly higher than those for a free chain except those at C(4) and C(5), and may be compensated using a slightly different k value. However, we will not examine further the free pentyl chain. The theoretical and experimental spectral densities agree qualitatively, with the exception of the theoretical values for C(4), which are too low. The effect of varying the jump rate k is shown in Fig. 5. All spectral densities of the chain deuterons in 5CB-d_{15} increase as k decreases. Therefore, one way of improving the fits for the spectral densities of C(4) is to reduce the jump rate k, but this is futile, since the fits at other carbon sites would drastically deteriorate. The possibility of different jump rates in the rate matrix $\bar{R}$ will be addressed later. The model also predicts frequency dependences in both $J_1(\omega)$ and $J_2(\omega)$ for the chain deuterons, as shown in

Fig. 6. The predicted frequency dependences of the ring deuteron spectral densities are shown in the same diagram. The frequency dependence in J_2 is less than that of J_1. This seems to qualitatively agree with the experimental data[1] given at three Larmor frequencies in the figure. The data at 15.3 MHz are obtained in our laboratory. Thus the model provides an explanation for the frequency dependences in the spectral densities, provided that the reorientation motion of the entire molecule has a $D_\perp$ value of less than about 5×10^7 s^{-1}.

It is noted above that the calculated spectral densities of C(4) deuterons are too low when a single k value is used in $\tilde{R}$. When the pentyl chain is restricted to conformations that start with a trans [Table 2(a)], the spectral densities of C(1) and C(2) deuterons are identical, and the variations in the spectral densities along the chain are very gradual. The large discrepancy in the spectral densities at C(4) seems to suggest that some jump rates in the rate matrix may be smaller. To explore the possibility of two sets of jump-rate constants in $\tilde{R}$, we assume that k_1''', k_2''' and k_3'' take a lower value. These jump-rate con-

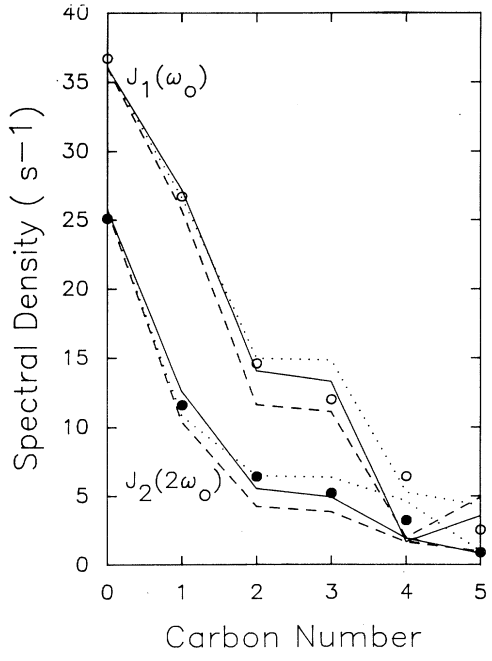

FIG. 4. Plot of theoretical spectral densities $J_1(\omega_0)$ and $J_2(2\omega_0)$ at 30.7 MHz and 302 K for 5CB-d_{15}. Carbon 0 refers to ring deuterons, while 1–4 refer to methylene deuterons on the pentyl chain. $\bar{P}_2=0.533$, $X_a/kT=1.8$, $X_{CC}/kT=0.54$, and $E_{tg}=3.5$ kJ/mol. Dashed curves are for a free pentyl chain, while the solid curves are for a chain in an anisotropic potential of mean torque. The adjustable parameters for these curves are $D_\parallel=7.6\times10^8$ s^{-1}, $D_\perp=4.5\times10^7$ s^{-1}, $D_R=2.2\times10^9$ s^{-1}, and $k=6\times10^{12}$ s^{-1}. The dotted curves are generated for a constrained chain with the same rotational diffusion constants but with two jump rate constants ($k=1.3\times10^{13}$ s^{-1} and another jump rate constant, see text). Open and closed symbols denote experimental data.

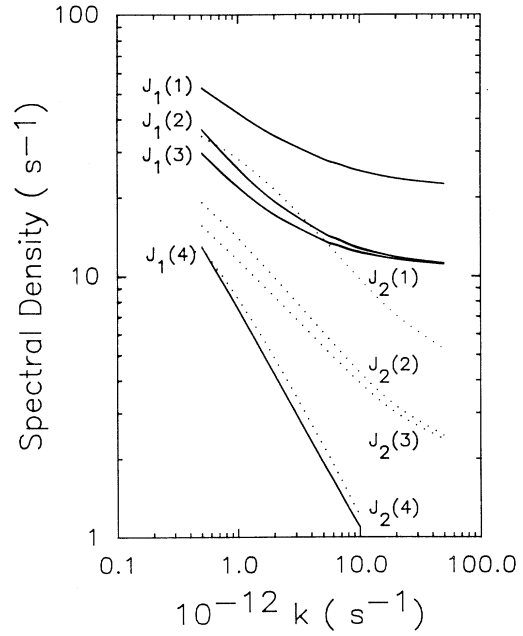

FIG. 5. Plot of theoretical spectral densities $J_1(\omega_0)$ and $J_2(2\omega_0)$ at 30.7 MHz and 302 K vs the jump rate k. Rotational diffusion constants are given in Fig. 4. The number within the brackets of J's refers to the carbon number.

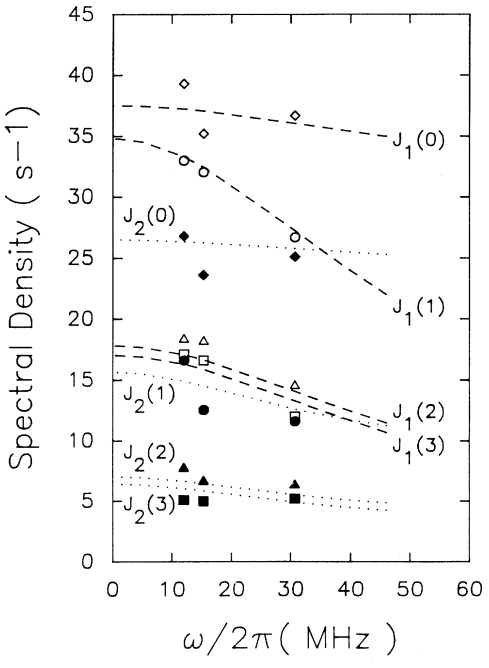

FIG. 6. Plot of theoretical spectral densities $J_1(\omega_0)$ (dashed lines) and $J_2(2\omega_0)$ (dotted lines) vs the Larmor frequency at 302 K using a single jump rate for 5CB-d_{15}. All parameters are listed in the caption of Fig. 4. The open symbols denote J_1, while the closed symbols denote the corresponding J_2. ◇, ○, △, and □ denote experimental data at 12, 15.3, and 30.7 MHz for carbon 0, 1, 2, and 3, respectively (carbon number also appears within brackets of J's).

stants affect interconversions that change the number of gauche linkages between two and three in the conformations involved in the transition (see Table II). The effect of lowering these rates is to raise all the calculated spectral densities, in particular those of C(4) deuterons. Without optimizing the fits between the calculated and experimental spectral densities of the chain deuterons, we show in Fig. 4 calculated spectral densities for a constrained chain using $k_1''' = k_2''' = k_3'' = 4 \times 10^{11}$ s^{-1} and all the remaining k's equal to 1.3×10^{13} s^{-1}. It would appear that one may satisfactorily reproduce the experimental data using two sets of jump-rate constants. If all the k_3's are set to zero to disallow three-bond motions, one again obtains identical spectral densities for the C(1) and C(2) deuterons.

To examine the temperature dependence of the spectral densities of chain deuterons in 5CB, we are limited by the available data[1] at different temperatures and frequencies. At 292 K, $X_a = 5.58$ kJ/mol and $X_{CC} = 1.68$ kJ/mol.[22] Using $\bar{P}_2 = 0.625$, $E_{tg} = 3.5$ kJ/mol, $D_\parallel = 6.8 \times 10^8$ s^{-1}, $D_\perp = 3.5 \times 10^7$ s^{-1}, and $D_R = 1.28 \times 10^9$ s^{-1}, $J_1^{(R)}(\omega_0)$ and $J_2^{(R)}(2\omega_0)$ at $\omega_0/2\pi = 30.7$ MHz are calculated from Eq. (26) to be 59.50 and 34.35 s^{-1}, respectively. In Fig. 7, the frequency dependences of the calculated spectral densities for the ring and C(1)-C(3) deuterons with $k = 4.7 \times 10^{12}$ s^{-1}, together with their experimental values at two Larmor frequencies are shown. Again, a qualitative resemblance between the theory and experimental data may be observed. Furthermore, the motional parameters, as expected, are found lower than those used at 302 K.

The purpose of this paper has been to present a model to describe correlated internal rotation in a pentyl chain of a liquid crystal. It has been demonstrated that the observed frequency and site dependences of the spectral densities for the chain deuterons of 5CB can be predicted qualitatively. We note, however, that fairly precise measurements of spectral density of motion as a function of temperature and frequency are required before a quantitative fit to the above model may be attempted.

An interesting article by Ferrarini *et al.* has recently appeared.[26] A master equation[12] was used to describe internal motions in 5CB. Though they explicitly considered a configuration-dependent rotational diffusion tensor, they still assumed that the overall and internal motions are independent of each other. Rather heavy computation procedures were required by these authors to accomplish configuration-dependent rotational diffusion tensors. Despite differences between their approach and the present work, these authors appeared to reach similar conclusions to ours.

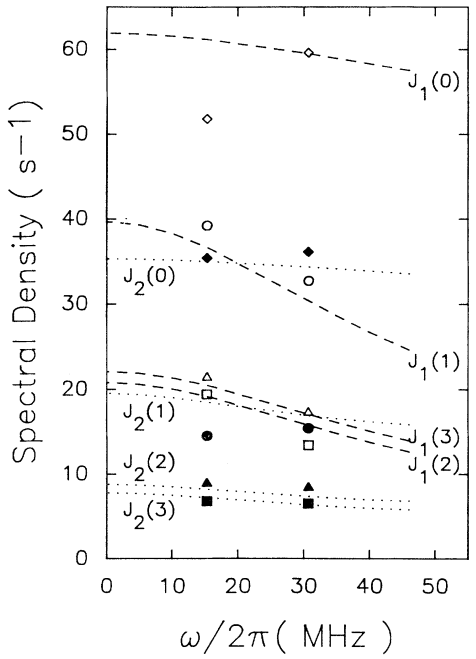

FIG. 7. Plot of theoretical spectral densities $J_1(\omega_0)$ (dashed lines) and $J_2(2\omega_0)$ (dotted lines) vs the Larmor frequency at 292 K for 5CB-d_{15}. $\bar{P}_2 = 0.625$, $X_a/kT = 2.3$, $X_{CC}/kT = 0.69$, and $E_{tg} = 3.5$ kJ/mol. The adjustable parameters are $D_\parallel = 6.8 \times 10^8$ s^{-1}, $D_\perp = 3.5 \times 10^7$ s^{-1}, $D_R = 1.28 \times 10^9$ s^{-1}, and $k = 4.7 \times 10^{12}$ s^{-1}. The open symbols denote J_1 while the closed symbols denote the corresponding J_2. ◇, ○, △, and □ denote experimental data at 15.3 and 30.7 MHz for carbon 0, 1, 2, and 3, respectively (carbon number also appears within brackets of J's).

ACKNOWLEDGMENTS

The financial support of the Natural Sciences and Engineering Council of Canada is gratefully acknowledged. We thank Dr. G. M. Richards for useful discussions and assistance in the numerical computations.

[1] P. A. Beckmann, J. W. Emsley, G. R. Luckhurst, and D. L. Turner, Mol. Phys. **50**, 699 (1983); C. R. J. Counsell, J. W. Emsley, G. R. Luckhurst, D. L. Turner, and J. Charvolin, *ibid.* **52**, 499 (1984); P. A. Beckmann, J. W. Emsley, G. R. Luckhurst, and D. L. Turner, *ibid.* **59**, 97 (1986).

[2] D. Goldfarb, R. Y. Dong, Z. Luz, and H. Zimmerman, Mol. Phys. **54**, 1185 (1985); R. Y. Dong and K. R. Sridharan, J. Chem. Phys. **82**, 4338 (1985); R. Y. Dong and G. M. Richards, J. Chem. Soc. Faraday Trans. II **84**, 1053 (1988); R. Y. Dong, Phys. Rev. A **42**, 858 (1990).

[3] T. M. Barbara, R. R. Vold, and R. L. Vold, J. Chem. Phys. **79**, 6338 (1983); T. M. Barbara, R. R. Vold, R. L. Vold, and M. E. Neubert, *ibid.* **82**, 1612 (1985).

[4] N. J. Heaton, Ph.D. thesis, University of Southampton, 1986; R. Y. Dong, J. W. Emsley, and J. Hamilton, Liq. Cryst. **5**, 1019 (1989).

[5] D. J. Wallach, J. Chem. Phys. **47**, 5258 (1967).

[6] Y. K. Levine, N. J. M. Birsdall, A. G. Lee, J. C. Metcalfe, P. Partington, and G. C. K. Roberts, J. Chem. Phys. **60**, 2890 (1974).

[7] R. E. London and J. Avitabile, J. Am. Chem. Soc. **99**, 7765 (1977); **100**, 7159 (1978).

[8]P. J. Flory, *Statistical Mechanics of Chain Molecules* (Interscience, New York, 1969).
[9]A. Tsutsumi, Mol. Phys. **37**, 111 (1979).
[10]R. J. Wittebort and A. Szabo, J. Chem. Phy. **69**, 1722 (1978).
[11]O. Edholm and C. Blomberg, Chem. Phys. **42**, 449 (1979).
[12]A. Ferrarini, G. Moro, and P. L. Nordio, Mol. Phys. **63**, 225 (1988).
[13]R. Y. Dong, J. Chem. Phys. **88**, 3962 (1988).
[14]J. W. Emsley, G. R. Luckhurst, and C. P. Stockley, Proc. R. Soc. London Ser. A **381**, 117 (1982); G. Q. Cheng and R. Y. Dong, J. Chem. Phys. **89**, 3308 (1988).
[15]P. L. Nordio and P. Busolin, J. Chem. Phys. **55**, 5485 (1971); P. L. Nordio, G. Rigatti, and U. Segre, *ibid.* **56**, 2117 (1972).
[16]C. F. Polnaszek, G. V. Bruno, and J. H. Freed, J. Chem. Phys. **58**, 3185 (1973); W. J. Lin and J. H. Freed, J. Phys. Chem. **83**, 379 (1979).
[17]R. R. Vold and R. L. Vold, J. Chem. Phys. **88**, 1443 (1988).
[18]G. R. Luckhurst and A. Sanson, Mol. Phys. **24**, 1297 (1972); C. F. Polnaszek and J. H. Freed, J. Phys. Chem. **79**, 2283 (1975); P. L. Nordio, G. Rigatti, and U. Segre, Mol. Phys. **25**, 129 (1973); A. Szabo, J. Chem. Phys. **72**, 4260 (1980); C. Zannoni, Mol. Phys. **38**, 1813 (1979); I. Dozov, N. Kirov, and M. P. Fontana, J. Chem. Phys. **81**, 2585 (1984); N. Kirov, I. Dozov, and M. P. Fontanta, *ibid.* **83**, 5267 (1985).
[19]R. Y. Dong and G. M. Richards, Chem. Phys. Lett. **171**, 389 (1990).
[20]A. Abragam, *Principles of Nuclear Magnetic Resonance* (Oxford University, London, 1961).
[21]B. Valeur, J.-P. Jarry, F. Geny, and L. Monnerie, J. Poly. Sci. **13**, 667 (1975); B. Valeur, L. Monnerie, and J. P. Jarry, *ibid.* **13**, 675 (1975).
[22]C. J. R. Counsell, J. W. Emsley, N. J. Heaton, and G. R. Luckhurst, Mol. Phys. **54**, 847 (1985).
[23]W. H. Press, B. P. Flannery, S. A. Teukolsky, and W. T. Vetterling, *Numerical Recipes* (Cambridge University, Cambridge, England, 1986).
[24]R. Y. Dong, Mol. Cryst. Liq. Cryst. **141**, 349 (1986).
[25]A. Ferrarini, P. L. Nordio, G. J. Moro, R. H. Crepeau, and J. H. Freed, J. Chem. Phys. **91**, 5707 (1989); R. W. Pastor, R. M. Venable, and M. Karplus, *ibid.* **89**, 1112 (1988); R. W. Pastor, R. M. Venable, M. Karplus, and A. Szabo, *ibid.* **89**, 1128 (1988).
[26]A. Ferrarini, G. J. Moro, and P. L. Nordio, Liq. Cryst. **8**, 593 (1990).